JEB™
Website : www.jeb.co.in
E-mail : editor@jeb.co.in

Journal of Environmental Biology

ISSN: 0254-8704 (Print)
ISSN: 2394-0379 (Online)
CODEN: JEBIDP

Depression internal solitary wave interaction with submerged obstacle

Chunling Wang[1], Lingling Wang[2]*and Hongwu Tang

[1]College of Water Conservancy and Hydropower Engineering, Hohai University, Nanjing, 210098, China

[2]State Key Laboratory of Hydrology-Water Resources and Hydraulic Engineering, Hohai University, Nanjing, 210098, China

*Corresponding Author E-mail: **wanglingling@hhu.edu.cn**

Publication Info

Paper received:
19 September 2015

Revised received:
27 April 2016

Re-revised received:
05 May 2016

Accepted:
23 June 2016

Abstract

The process of depression internal solitary wave interaction with submerged plate has been successfully stimulated in the present study. The characteristics of internal solitary wave interact with submerged plate have been reported. The results showed that both transformation and reflection were found in the wave-plate interaction. For reflected wave, the wave amplitude and wave energy obeyed logarithmic law with no dimensional blocking parameter. For transmitted wave, wave amplitude and wave energy followed exponential rule with the blocking parameter. The reflected and transmitted waves showed the same wave amplitude and wave energy, while the blocking parameter was nearly 0.8.

Key words

Internal solitary wave, Submerged plate, Wave amplitude, Wave energy

Introduction

Internal solitary wave (ISW), the fluctuation of interface, exists widely in a stratified fluid. This stratification is due to different temperature, salinity or other reasons. ISWs play a significant role in oceans and in some deep lakes. In oceans, ISWs generally have large amplitude and may generate powerful shear in destroying undersea equipment and threaten a submarine, such as the disaster of USA "sharks" nuclear submarine. It is well known that fluid stratification is harmful in lakes. The turbulence caused by ISWs can make stratified fluid mixing and improve the water environment. Meanwhile, ISWs also survive as an important mechanism for energy exchange and substance transportation.

In natural environment, internal solitary waves (ISWs) interact with submarine slope and bottom topography in variable forms such as rigid, sill, shelf and basin. Many field observations have indicated the turbulence caused by wave-topography interaction, which accelerates the vertical mixing of water in the coastal oceans (Bourgault *et al.*, 2003; Chen *et al.,* 2008, Kozlov *et al.,* 2014). Because turbulence diffusion has a very important effect on hydrodynamics, many researchers are focusing on describing the characters of ISWs on variable topography (Kozlov *et al.*, 2014). Their study suggested that the source of these packets is governed by the intense dynamics of the frontal zone in the tidal cycle over local complex bottom.

Helfrich *et al.* (1984) investigated ISW in a two-layer system at variable water depth. The experimental results indicated that several reversed polarity might have emerged as the upper layer thickness equal to the bottom one. Later on, ISWs propagation over the bottom topography was examined by a combination of theoretical modeling and laboratory experiment (Helfrich and Melville, 1986). Interaction between internal solitary wave and triangular obstacle were studied by Chen's (2007, 2008). The results showed that the overall performance depended on the relative height of the obstacle and ratio of upper layer and bottom layer thickness. ISWs propagation over trapezoidal topography were reported by Ming-Huang Cheng (2010). The author opined that waveform inversion occurred as crest-to-trough ratio at a

specific location changed from much small than unity at the incident stage to greater than unity on the plateau, where upper layer was thicker than the bottom one. ISW interaction with step topography was studied by Tatiana Talipova *et al.* (2013). They supposed that wave energy dissipation was close to the height of step and the maximum dissipation rate is about 50%. Barad and Fringer (2010) applied DNS method to simulate ISW interaction with slope, a density intrusion was found in the wave-topography interaction. This phenomenon was confirmed later by a combination of field observation and simulation (Pomar *et al.,* 2012). Investigation of Richardson number by Barad and Fringer (2010) indicated that wave breaking might be initiated through a combination of enhanced shear at the bottom layer and static instability associated with wave overturning above the topography. Bourgault (2014) used hydrodynamic model and sediment model simulated sediment re-suspension caused by ISWs. This was further confirmed that ISW is one of the effective mechanisms for off shore dispersal of muddy sediments (Chen *et al.,* 2008).

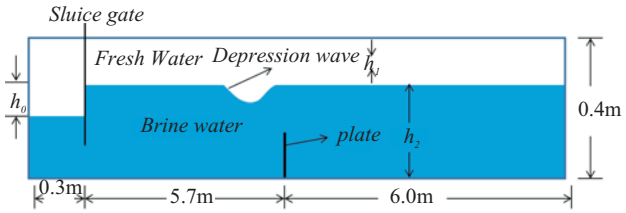

Fig. 1: Sketch of computational domain and ISW generation method (ISWs propagating from left to right)

Experimental and simulated tests on ISWs passing through a submerged topography were extensively studied and blocking parameters were used to describe ISW blocking. Selected examples are listed in Table 1. These studies have been usually carried on trianglular or trapezoidal topography as obstacles. However, at many places, especially in oceans, the obstacle can be simplified as a plate where its horizontal-thickness is considerably smaller than wavelength, such as submarine ridge. In this situation, the wave propagation and wave energy dissipation were mainly determined by ridge-height. In the present study, different height plates were employed to interact with ISWs. The detailed process of wave-obstacle interaction has been

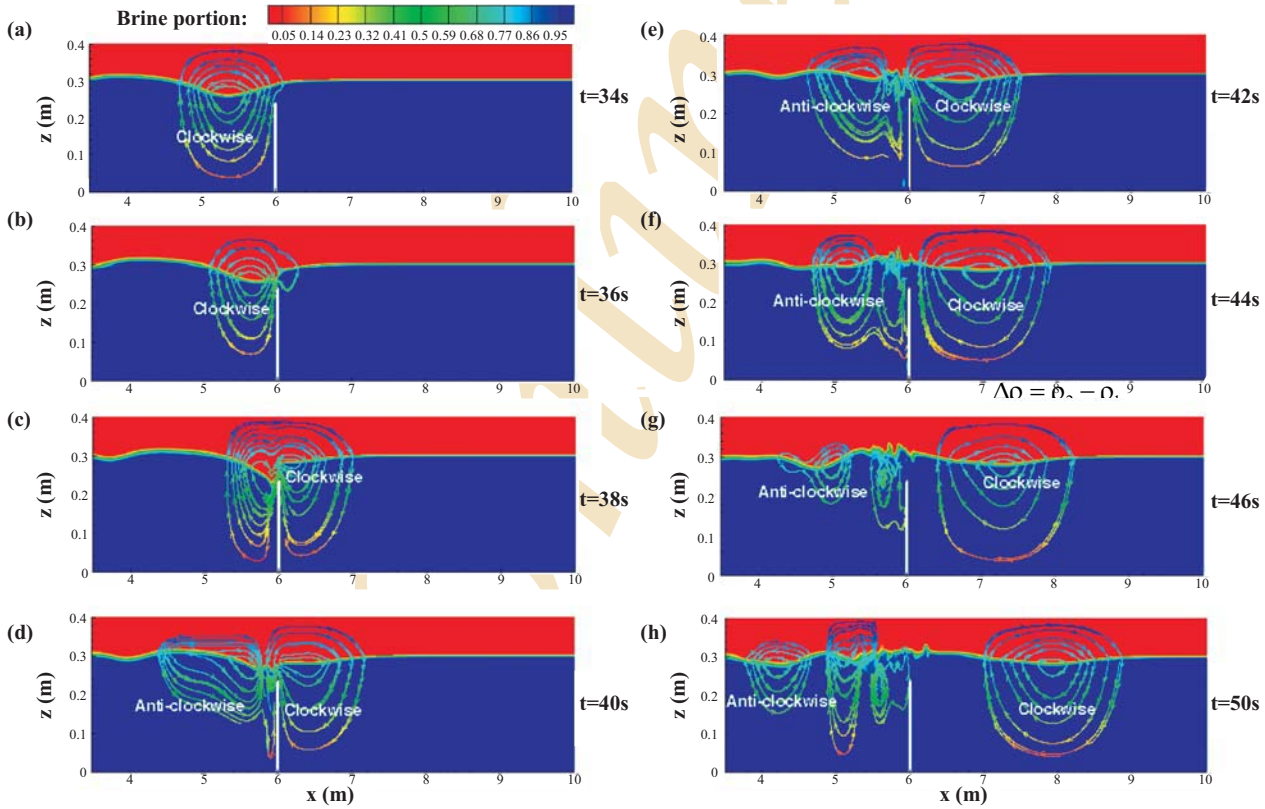

Fig. 2 : Process of depression ISW passing plate (hob=24cm,ho=10cm)

Table 1: Examples of experimental and simulated work on ISW moving over submerged obstacles

Wave type	Experiment or simulation	Shape of obstacle	Blocking	References parameter
Elevation	Experimental	Trapezoid	B=0.7	Helfrich (1984)
Depression	Experimental	Trapezoid	---	Kao *et al.* (1985)
Elevation	Experimental	Triangle	B=0.6~1.6	Wessels and Hutter (1996)
Depression	Experimental	Triangle Trapezoid	B=0.6~1.4	Michallet (1999)
Depression	Experimental	Triangle	ξ =3.2~0.8	Sveen *et al.* (2002)
Depression	Experimental	Triangle	ξ =0.3~1.2	Chen (2007)
Elevation		Semicircle	B=0.25~1.0	
Depression	Simulation & observation	slope	---	Bourgault (2014)

Table. 2 : Examples of experimental and simulated work on ISW moving over submerged obstacles

Cases	h_0/cm	h_1/cm	h_2/cm	h_{ob}/cm	h_0/cm
Case1	10	10	30	16	k_{in}=0.31
Case2	10	10	30	18	k_{in}=0.36
Case3	10	10	30	20	k_{in}=0.43
Case4	10	10	30	22	k_{in}=0.54
Case5	20	10	30	16	k_{in}=0.54
Case6	20	10	30	18	k_{in}=0.63
Case7	10	10	30	24	k_{in}=0.72
Case8	20	10	30	20	k_{in}=0.75
Case9	20	10	30	22	k_{in}=0.94
Case10	10	10	30	26	k_{in}=1.08
Case11	10	10	30	28	k_{in}=2.17
Case12	20	10	30	24	k_{in}=1.25
Case13	20	10	30	26	k_{in}=1.88
Case14	20	10	30	28	k_{in}=3.76

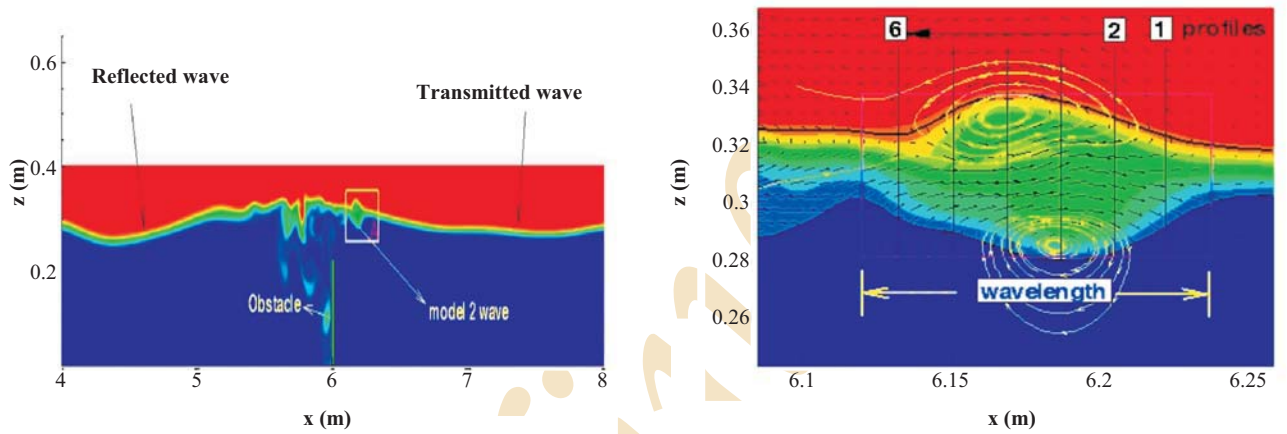

(a) Interaction of depression wave with plate

(b) Velocity field of zone A and location of measured profiles

Fig. 3 : Mode 2 ISWs generated from wave-obstacle interaction (profile 1 to profile 6 represent the location of velocity profiles that will be discussed in section 3.4)

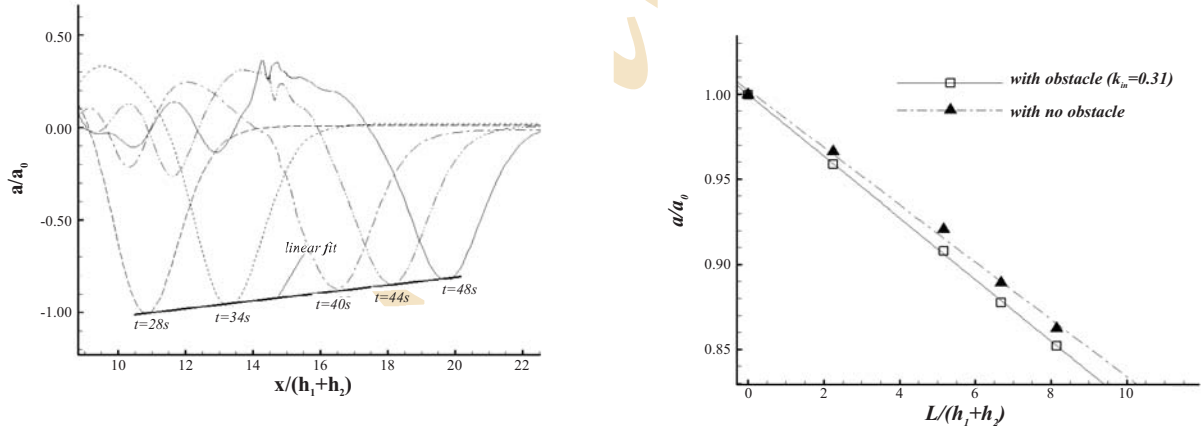

(a) Wave amplitude damping (k_{in} = 0.31)

(b) Normalized wave amplitude

Fig. 4 : ISW amplitude decaying along the flume

depicted. Wave amplitude damping and energy reducing issues also have been discussed.

Materials and Methods

Numerical wave flume : A series of ISWs can be generated in a numerical wave tank. The numerical wave flume having 12 m in length with a rectangular cross-section (0.5mx0.4m) in width and height was used in this numerical experiment (Fig.1). The thickness of upper layer was h_2 and h_o was step-depth. The plate was located at x=6m. "Step method", which was extensively used in many experiments (Chen, 2007; Ming-Huang and John, 2010; Zhu *et al.,* 2014) to generate ISWs. The step-like distribution of brine water showed initial status (the left part of flume in Fig. 1).

Computational approach : A 3D coherence model, which is extensively used in many fields, was applied to simulate wave-obstacle interaction in the present study. The details of the coherence model refer to Lu *et al.,* 2011; Zhu *et al.,* 2014. A self-developed FORTRAN code was applied in this study. The solving of governing equations and the model verification was according to Zhu *et al.* (2014). The initial pressure was hydrostatic and initial velocity was 0 m/s; the upper and lower-layer densities were 998 and 1030 kg m^{-3} respectively. The no-slip bottom and sidewall boundary were applied. The inflow boundary was a rigid wall and the Sommerfeld radiation condition was applied at the outflow boundary to reduce wave reflection.

Results and Discussion

Fourteen cases were designed to investigate wave-obstacle interaction. The details of the simulation cases are listed in Table 2.

Process of wave-obstacle interaction : While the lower layer depth was larger than the upper layer in a stratified water body, only depression type ISWs were found. This section examined the interaction of depression wave with plate. An important parameter, i.e., the wave-obstacle encounter is the blocking parameter. For convenience of calculation, k_{in} was selected to quantify the degree of ISW blocking. The expression of k_{in} is as follows (Vlasenko and Hutter, 2013):

$$k_{in} = a/(h_2 - h_{ob}) \quad (1)$$

where α is incident wave amplitude; h_2 is lower layer thickness; and h_{ob} is plate-height.

The process of wave-obstacle interaction has been revealed. Fig. 2 (a-h) shows the time series of wave-obstacle encounter. The incident waveform was measured t=30s on (Fig. 2a). At this time, ISW did not interact with the obstacle and the vortex was clockwise. At t=36s front of the incident wave began to show deformation and the vortex began to overcome the plate (Fig. 2b). Two seconds later (Fig. 2c), ISW deformation intensified and the interface washed down along the plate. In the meantime, the vortex was divided into two parts: the left one and the right one (Fig. 2c).

At t=40s, the sharp wave-valley moved upward and divided the vortex into two separate parts. The vortex on the left of the plate changed from clockwise to anti-clockwise. From t=42s to t=46s, incident wave gradually overcame the plate and the transmitted and reflected waves were observed at t=46s (Fig. 2g). Besides, a series of irregular vortexes were generated on the left of the obstacle during the process of interaction.

Wave-obstacle interaction caused water mixing and the mixing just emerged on the left of plate (Fig. 3). In stratified lakes, the mixing was useful for improving environment in water. During wave-obstacle interaction, a moving “ball” might be generated. The “ball” followed the transmitted wave i.e. the so called mode 2 wave (Fig. 3a). The “ball” nearly showed no fluctuation in vertical direction, it just moved along the interface. Therefore, it might be one of mechanisms responsible for substance transport near the interface. Mode 2 wave was different from depression wave or elevation wave. In mode 2 wave, lower iso-surface formed an elevation wave and a thicker iso-surface formed a depression wave (Fig. 3b).

Blocking parameter with ISW amplitude and energy : Different height plates have different influences in wave-obstacle interaction, and the different plates correspond to the variable blocking parameters. So, the influence of blocking parameter has been discussed in this section.

Fig. 4a shows the normalized waveforms from t=28s to t=48s. All the wave amplitudes were normalized with incident wave amplitude a_0, and x was normalized with total water depth. It is clear that wave amplitude followed a linear collapse when k_{in} was 0.31.

Fig. 4b shows comparison of wave amplitude, where triangle symbols represent ISW amplitude damping with no obstacle and square symbols represent ISW amplitude damping with blocking parameter near 0.31. Wave propagation distance L and wave amplitude normalized with

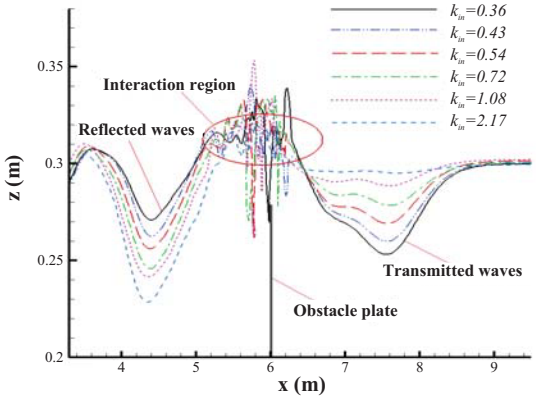

Fig. 5 : Reflected and transmitted ISWs with blocking parameters

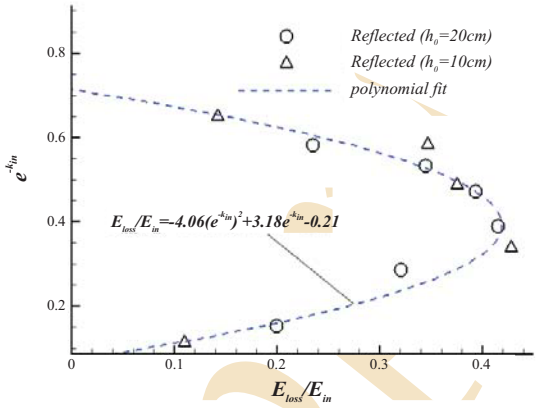

Fig. 7 : Wave energy dissipation with k_{in}

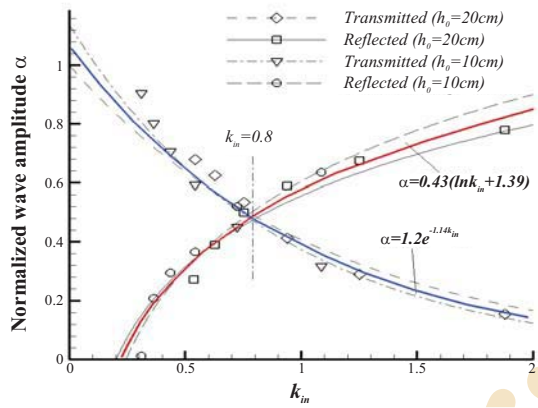

(a) Wave amplitude versus k_{in}

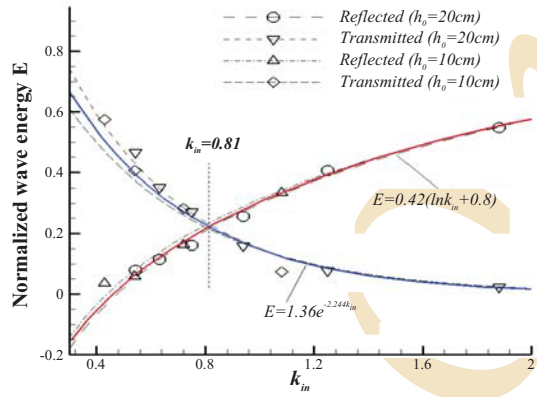

(b) Wave energy versus k_{in}

Fig. 6 : Amplitude damping and wave energy dissipation

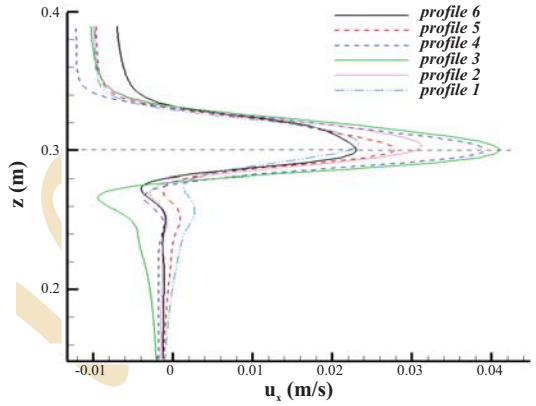

(a) Velocity profiles (profile 1 to profile 6) in Fig. 3b

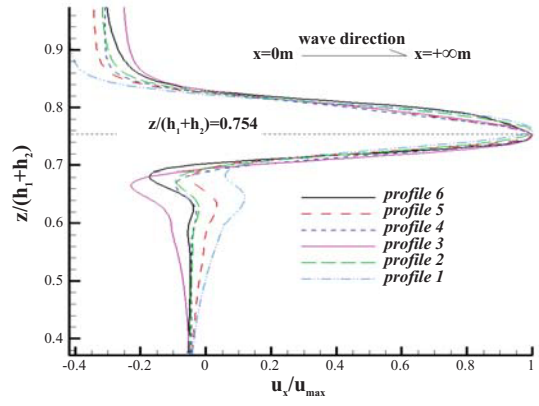

(b) Normalized velocity profiles (profile 1 to profile 6)

Fig. 8 : Velocity profiles and normalized velocity profiles of mode2 ISW

the total water depth and incident wave amplitude respectively. For k_{in}=0.3, the wave amplitude damping was very close to that amplitude damping with no obstacle. The influence of submerged plate was ignored.

Wave-obstacle interaction composed of three parts: transmission, reflection and losing (including transformation and dissipation). Fig. 5 shows changing of the reflected wave amplitude and transmitted wave amplitude, where k_{in} is a variable. From Fig. 5, we can know that in the range of k_{in}=(0.36~2.17), reflected wave amplitude increased and the transmitted one decreased. Transmitted wave amplitude was quite small that could be ignored, where k_{in} was 2.17. Wave blocking parameter k_{in} is a quantity to describe wave-obstacle interaction degree. The relationship between k_{in} and wave amplitude as well as wave energy is displayed in Fig. 6. in which α is normalized wave amplitude and E is normalized wave energy. Wave energy was calculated by the following formula (Wessels and Hutter, 1996) :

$$E = \frac{1}{2} g\Delta\rho \int_{x_1}^{x_2} f^2(x,t)dx \qquad (2)$$

where, $\Delta\rho = \rho_2 - \rho_1$; g is the gravitational acceleration, f(x,t) is the vertical distribution of interface displacement along the channel for a fixed time, x_1 and x_2 are locations at the left and right of a wave train.

From the figure, it may be seen that transmitted wave amplitude and wave energy obey exponential collapse with blocking parameter k_{in}. Reflected wave amplitude and energy followed logarithmic law with k_{in}. At approximately k_{in}=0.8, reflected wave amplitude (and energy) was equal to transmitted wave amplitude (and energy). That means reflection and transmission had equal weight when k_{in} was 0.8.

Energy losing : It is well know that wave amplitude damping is due to loss of energy. The loss of wave energy was determined mainly by blocking parameter. In this section, the relationship between lost energy and blocking parameter was determined by the following formula :

$$E_{loss} = E_{in} - E_{re} - E_{tr} \qquad (3)$$

where, E_{loss} is the energy dissipation; E_{in} is incident wave energy; E_{re} is the reflected wave energy and E_{tr} is the transmitted wave energy. Wave energy was calculated by the formula given by Chen *et al.* (2008). Fig. 7 shows the energy losing and blocking parameters. The wave energy was normalized with incident wave energy. It was noted that wave energy losing followed a polynomial law with blocking parameter and the relationship was expressed as:

$$\beta = a_0\alpha^2 + a_1\alpha + a_2 \qquad (4)$$

where, $e^{-k_{in}}$ represents energy losing rate E_{loss} / E_{in}, parameters a_0, a_1 and a_2 were constants with values -4.06, 3.18 and -0.21 respectively in the present study. The energy losing rate increased with e-kin and later on decreased. Its maximum value (about 43%) appeared at $e^{-k_{in}} \approx 0.4$ (Fig.7b). This means that there exists a right obstacle height, which dissipates the wave energy most efficiently. In wave-obstacle interaction, a large portion of dissipated wave energy was used to generate turbulence. The turbulence strengthened shear and reduced the stability of hydraulic structure. The present study provides an available reference for hydraulic structure design near the similar topography.

Velocity structure of mode 2 waves : In section 3.1, a mode 2 wave was investigated in the process of wave-obstacle interaction (Fig. 3). Jet-like velocity structure was found in the mode 2 wave. Velocity field is important because it is responsible for substance transport. In order to investigate the velocity of mode 2 ISW, six velocity profiles were recorded (Fig. 3b). These profiles were located in the front (x=6.220m and 6.202m), middle (x=6.184m and 6.166m) and rear of the wave (x=6.148m and 6.130m) respectively.

Velocity profiles and its normalized profiles are displayed in Fig. 8a and b, respectively. The maximum velocity at profile 1 to 6 was 0.022 m sec^{-1}, 0.028 m sec^{-1}, 0.038 m sec^{-1}, 0.04 m sec^{-1}, 0.031 m sec^{-1} and 0.022 m sec^{-1} respectively. From profile 1 to profile 4, the maximum velocity increased. From profile 4 to 6, the maximum velocity decreased. This means, maximum velocity of mode 2 waves was in the core. It is about 35% of wavelength distance from the front of mode 2 wave.

Normalized with its corresponding maximum velocity, normalized vertical profiles of velocity is in x direction (Fig. 8b), all profiles generally similar collapse and maximum velocity was located near the interface ($z \approx 0.3$m). Taking average of all the velocity profiles, it was found that average velocity in upper layer and lower layer was negative. The averaged velocity was positive just in the "ball" and was different to depression or elevation ISW. For unique velocity structures, mode 2 ISW might be one of mechanism of the substance transportation.

The present study revealed that ISWs interacted with

vertical plate obstacle which differed from triangle and trapezoid topographies. The main conclusions are as follows:

(1) Depression ISWs interact with submerged plate obstacle can be divided into 4 stages. For reflected wave, wave energy and amplitude followed an exponential law with parameter k_{in}. For transmitted wave, wave amplitude and energy obeyed exponential attenuation rule with k_{in}. With the growth of obstacle height, wave energy dissipation usually increased and later on decreased. The maximum energy dissipation occurred around k was 0.9.

Mode 2 ISWs have been discovered during the interaction. The unique velocity structure determined that mode 2 wave might be a mechanism responsible for substance transport in interface.

Acknowledgments

This work was supported by the National Natural Science Foundation of China (Grant No. 51479058 and 51309085), the State Key Program of the National Natural Science of China (Grant No. 51239003), the 111 Project (grant no. B12032), the Fundamental Research Funds for the Central Universities (2014B36114) and the Innovation Project of the Scientific Research for College Graduates of Jiangsu Province (KYLX_0467).

References

Bourgault, D. and D.E. Kelley: Wave-induced boundary mixing in a partially mixed estuary. *J. Marine Res.*, **61**, 553-576 (2003).

Barad, M.F and O.B. Fringe : Simulations of shear instabilities in interfacial gravity waves. *J. Fluid Mech.*, **644**, 61-95 (2010).

Chen, C.Y., J.R.C. Hsu, M.H. Cheng and C.W. Chen : Experiments on mixing and dissipation in internal solitary waves over two triangular obstacles. *Environ. Fluid Mecha.*, **8**, 199-214 (2008).

Chen, C.Y. : An experimental study of stratified mixing caused by internal solitary waves in a two-layered fluid system over variable seabed topography. *Ocean Engineering*, **34**, 1995-2008 (2007).

Cheng, M.H. and J.R. Hsu : Laboratory experiments on depression interfacial solitary waves over a trapezoidal obstacle with horizontal plateau. *Ocean Engineering*, **37**, 800-818 (2010).

Helfrich, K.R. and W.K. Melville : On long nonlinear internal waves over slope-shelf topography. *J. Fluid Mech.*, **167**, 285-308 (1986).

Helfrich, K.R., W.K. Melville and J.W. Miles : On interfacial solitary waves over slowly varying topography. *J. Fluid Mech.*, **149**, 305-317 (1984).

Kao, T.W., F.S. Pan and D. Renouard: Internal solitions on thepycnocline: generation, propagation, shoaling and breaking over a slope, *Fluid Mechanics*, **159**, 19–53 (1985).

Kozlov, I., D. Romanenkov, A. Zimin and B. Chapron : SAR observing large-scale nonlinear internal waves in the White Sea. *Remote Sens. Environ.*, **147**, 99-107 (2014).

Lu, J., L.L.Wang, H. Zhu and H.C. Dai : Large eddy simulation of water flow over series of dunes. *Water Sci. Engin.*, **4**, 421-430 (2011).

Michallet, H. and G.N. Ivey: Experiments on mixing due to internal solitary waves breaking on uniform slopes. *Geophys. Res.,* **104**, 13467-13477 (1999).

Pomar, L., M. Morsilli, P. Hallock and B. Bádenas : Internal waves, an under-explored source of turbulence events in the sedimentary record. *Earth-Science Reviews*, **111**, 56-81 (2012).

Talipova, T., K. Terletska, V. Maderich, I. Brovchenko, K.T. Jung, E. Pelinovsky and R. Grimshaw : Internal solitary wave transformation over a bottom step : Loss of energy. *Physics of Fluids (1994-present)*, **25**, 032-110 (2013).

Vlasenko, V.I and K. Hutter : Transformation and disintegration of strongly nonlinear internal waves by topography in stratified lakes. *In Annales Geophysicae*, **20**, 2087-2103 (2002).

Wessels, F., K. Hutter : Interaction of internal waves with a topographic sill in a two-layered fluid. *J. Physical Oceanography*, **26**, 5-20 (1996).

Zhu, H., L.L. Wang and H.W. Tang: Large-eddy simulation of the generation and propagation of internal waves, *J. China Phys., Mech. Astron.*, **57**, 1128-1136 (2014).